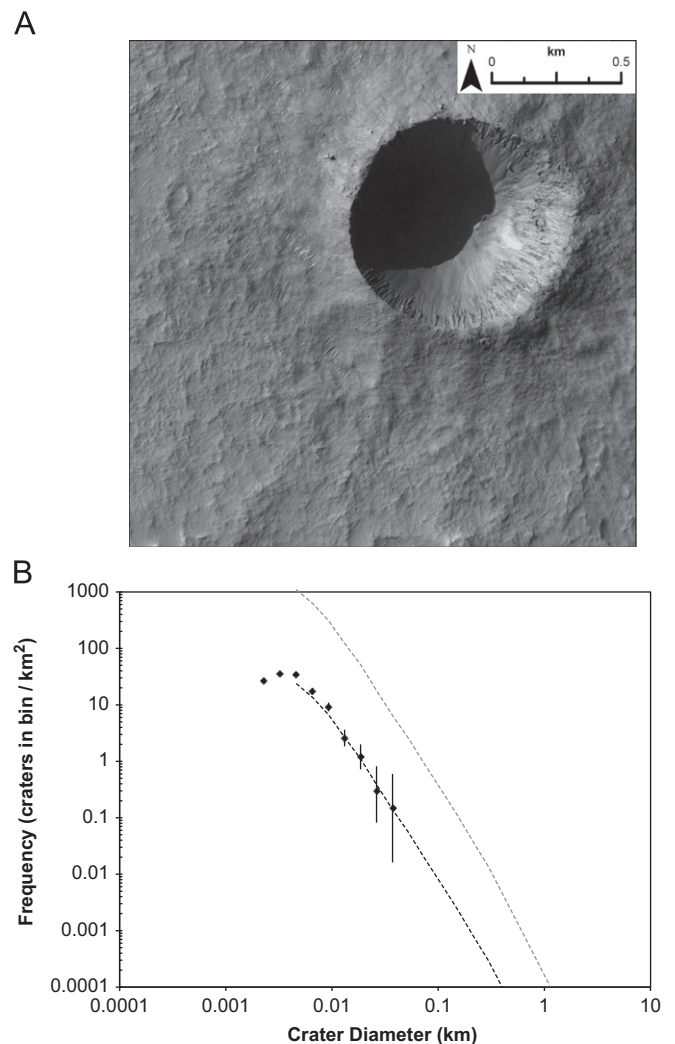


**Fig. 8.** (A) An unnamed 4.3-km diameter crater is found in Tyrrenhia Terra (23.9°S, 94.8°E). No evidence of latitude-dependent mantling is observed. Portion of HiRISE: PSP\_008030\_1560. (B) A crater count revealed 4355 craters on 6.0 km<sup>2</sup> of near-rim deposits surrounding the unnamed crater (23.9°S, 94.8°E). Isochrons of Hartmann (2005) indicate a best-fit age of 18.1 Ma. The grey dashed line marks the Early Amazonian boundary of Hartmann (2005).

areas, and the surrounding terrain. Finally, a collection from the mid-latitudes is considered (Figs. 7–16). Variations in latitude, crater-retention age, and the presence or absence of superposed mantling deposits at these locations provide constraints on the history of latitude-dependent mantling.

#### 4.1. Equatorial rayed craters

The distinctiveness of lunar crater rays arises from compositional and maturity differences with the background terrain (e.g., Hawke et al., 2004). Thermal inertia (TI) differences with surrounding terrain (e.g., low TI rays) are thought to be responsible for the thermophysical distinctiveness of martian rays (McEwen et al., 2005; Tornabene et al., 2006; Preblich et al., 2007). Therefore, rays are most apparent in nighttime infrared data (Christensen et al., 2004). The distribution of identified rayed craters (Tornabene et al., 2006) suggests that the occurrence (or persistence) of rays is dependent on substrate. Intermediate to high background thermal inertia and intermediate albedo appear to be important criteria regarding the distinguishability of rays (see global maps of Mellon et al., 2000 and Putzig et al.,



**Fig. 9.** (A) An unnamed 0.8-km diameter crater is found in Terra Sabaea (24.9°S, 49.4°E). No evidence of latitude-dependent mantling is observed. Portion of HiRISE: PSP\_009983\_1550. (B) A crater count revealed 860 craters on 6.5 km<sup>2</sup> of near-rim deposits surrounding the unnamed crater (24.9°S, 49.4°E). Isochrons of Hartmann (2005) indicate a best-fit age of 5.8 Ma. The grey dashed line marks the Early Amazonian boundary of Hartmann (2005).

2005). This is consistent with most of the Tornabene et al. (2006) detections occurring in equatorial volcanic terranes.

Thila (Fig. 2), Naryn (Fig. 3), and Dilly (Fig. 4) all preserve crater rays that are visible in thermal infrared data (Tornabene et al., 2006). These morphologically fresh craters are located in the equatorial regions near Elysium (Fig. 1). Detailed crater counts on near-rim deposits to date the formation of these craters (Fig. 2(B), Fig. 3(B), Fig. 4(B)) reveal ages that vary by more than a factor of ten. The crater retention ages of Thila, Naryn, and Dilly are 23.1, 2.1, and 34.4 Ma, respectively. A study by Hartmann et al. (2010) estimated the age of Naryn as “a few Myr to 20 Myr.” These ages are consistent with very low erosion rates (Golombek and Bridges, 2000) and the general absence of very late Amazonian-aged glacial modification at these latitudes and longitudes (Kreslavsky and Head, 2006; Head and Marchant, 2009).

#### 4.2. High-latitude polygonalized craters

In the higher latitude region where polygonally patterned ground is pervasive (e.g., Mangold, 2005; Levy et al., 2009), we examined two young craters and their near-rim deposits. One crater (Fig. 5) is located at 55.6°S, while the other (Fig. 6) is